Article

Not peer-reviewed version

Stimuli-Sensitive Polymeric Micelles Formulations Enhance the Cytostatic Effect against the Leukemia Cells via “Aikido” Principle Realization

Igor D. Zlotnikov , Alexander A. Ezhov , Natalia Vladimirovna Dobryakova , Elena V. Kudryashova *

Posted Date: 2 February 2024

doi: 10.20944/preprints202402.0157.v1

Keywords: glutathione sensitivity, tumor targeting, polymeric micelles, doxorubicin, non-target toxicity

Article

Disulfide Cross-Linked Polymeric Redox-Responsive Nanocarrier Based on Heparin, Chitosan and Lipoic Acid Improved Drug Accumulation, Increased Cytotoxicity and Selectivity to Leukemia Cells by Tumor Targeting via "Aikido" Principle

Igor D. Zlotnikov [1], Alexander A. Ezhov [2], Natalia V. Dobryakova [1] and Elena V. Kudryashova [1,*]

[1] Faculty of Chemistry, Lomonosov Moscow State University, Leninskie Gory, 1/3, 119991 Moscow, Russia; zlotnikovid@my.msu.ru (I.D.Z.)
[2] Faculty of Physics, Lomonosov Moscow State University, Leninskie Gory, 1/2, 119991 Moscow, Russia; alexander-ezhov@yandex.ru
* Correspondence: helenakoudriachova@yandex.ru (E.V.K.)

Abstract: We have developed a nanogel formulation of anticancer drugs based on chitosan, heparin grafted with lipoic and oleic acids, that can release the cytotoxic cargo (doxorubicin) in response to external stimuli, such as increased glutathione concentration – a hallmarks of cancer. Natural polysaccharides (heparin and chitosan) provide the pH sensitivity of the nanocarrier: the release of doxorubicin (Dox) is enhanced in a slightly acidic environment (tumor microenvironment). Fatty acid residues are necessary for the formation of nanoparticles (micelles) and solubilization of cytostatics in a hydrophobic core. Lipoic acid residues provide formation of a labile S-S cross-linking between polymer chains (the first variant) or covalently attached doxorubicin molecules through glutathione-sensitive S-S bridges (the second variant) – both determine Redox sensitivity of the anticancer drugs carriers stable in blood circulation and disintegrate after intracellular uptake in the tumor cells. The release of doxorubicin from micelles occurs slowly (20% / 6h) in an environment with a pH of 7.4 and the absence of glutathione, while in a slightly acidic environment and in the presence of 10 mM glutathione, the rate increases up 6 times, with an increase in the effective concentration up to 5 times after 7 h. The permeability of doxorubicin in nanogel formulations (covalent S-S crosslinked and not) into Raji, K562, A875 cancer cells was studied using FTIR, fluorescence spectroscopy and confocal laser scanning microscopy (CLSM). We have shown dramatic improved accumulation, decreased efflux and increased cytotoxicity compared to doxorubicin control with three tumor cell lines Raji, K562, A875. At the same time, cytotoxicity and permeability for non-tumor cells (HEK) is significantly lower, increasing selectivity index against tumor cells by several times.

Keywords: glutathione sensitivity; tumor targeting; polymeric micelles; doxorubicin; non-target toxicity

1. Introduction

In modern biomedicine, one of the urgent tasks is to create targeted drug delivery systems [1–7], this is especially true for Oncological diseases, which require long-term treatment with high dosages. Therefore, in order to improve the quality of life, it is important to find optimal and effective methods of chemotherapy [8]. Existing medical strategies mostly have one common drawback – high non-target toxicity (especially heart, liver, kidneys) [9,10]. Therefore, in order to improve the quality of life, it is important to find optimal and effective methods of chemotherapy [8]. Existing medical strategies mostly have one common drawback – high non-target toxicity (especially heart, liver, kidneys) [9,10]. To increase the selectivity of cytostatics against tumors we developed the drug delivery systems based on polymeric nanoparticles (micelles). A key aspect of these delivery systems is the attachment specific label or trigger to the molecular container [11–18]. Besides the approaches base on the actively targeting tumors cells via specific receptors (folic and sialic acid residues, biotin,

 doi:10.20944/preprints202402.0157.v1

antibodies, peptides, glucose transporters etc [19]), in the case of tumors the following differences from normal tissues can be taken in the attention [6,19–32]: 1) a slightly acidic environment (pH 5.5-6.5), 2) a local increase in temperature, 3) an increase in blood viscosity (including local thrombosis), 4) altered morphology of cancer cells and increased permeability (leaky membrane), and 5) increased concentrations of reduced glutathione (GSH).

The creation of "smart" polymeric nanogel particles make it possible to increase the effectiveness and reduce the toxicity of antitumor drugs [24,25,27,31,33,34]. In this paper, we developed stimuli-sensitive smart polymeric micelles based on chitosan or heparin grafted with fatty acid with function of tumor targeting and delivery of the model cytostatic, doxorubicin (Dox).

The pH sensitivity in polymeric micelles is provided by chitosan [31], a biocompatible, biodegradable polymer with a pK_a of the amino group of the order of 6.2-6.4 units. In a weakly acidic medium corresponding to the tumor microenvironment, chitosan amino groups are protonated and the micelle structure is loosened with the drug release. This effect is especially evident when the drug molecule itself is similarly charged: for example, Dox is positively charged at pH < 8, which causes repulsion from polymer chains in the tumor medium.

Thermal sensitivity in smart particles is provided by polymer chains (thermally dependent gels or thermogels, hydrogels [35–38]) of chitosan or heparin, which undergo changes in the microstructure with an increase in temperature from 37 to 40-42 °C.

Patients with oncological diseases have a significantly increased risk of micro-thrombosis [39–41], which secondarily provokes problems with the cardiovascular system, brain, thromboembolism, etc. Indeed, cancer determines the formation of chronic coagulation activation due to the production of procoagulant substances by tumor cells (tissue coagulation factor, cysteine transpeptidase, etc.), which increase thrombotic activity, moreover, idiopathic thromboembolism (Trousseau's syndrome) is often associated with cancer. It has also been shown that in the presence of a number of tumor cell lines, the antithrombotic activity of heparin (antithrombin activator) is neutralized [42]. Therefore, we suggest using the antithrombotic agent heparin as the main component of polymeric micelles to reduce blood density and prevent the risk of thrombosis [43–46].

The other important differences between cancer cells and normal ones include morphological features [47]: an enlarged nucleus, an increased ratio of nucleus and cytoplasm, altered membrane, hyperchromasia and abnormal chromatin distribution – in other words, cancer cells are "defective" and this can be used to deliver targeted drugs.

Besides, RedOx sensitivity, namely glutathione (GSH) sensitivity of polymeric nanoparticles, ensures the presence of labile disulfide bonds between polymer chains or between polymer and drug. GSH is the most important antioxidant in cells [48,49]. GSH is found in all cell compartments in millimolar concentrations (1-10 mM). In the case of cancer, GSH plays both a protective and pathogenic role. It is involved in the detoxification of carcinogens, and changes in this pathway can have a profound effect on cell viability. An increased concentration of GSH accumulates in cancer cells, which may cause resistance to antitumor drugs (cytostatics). Smart micelles use this feature of cancer cells: GSH as a trigger causes accelerated release of cytostatic.

Thus, the present work is aimed at the development of polymeric smart micelles combining the properties of pH-, thermo-, stimulus-sensitivity to tumor microenvironment. This will potentially increase the effectiveness of chemotherapy and reduce the systemic burden on the body.

Currently, the use of smart delivery systems for the treatment of oncological diseases will increase the effectiveness of therapy for various types of cancer, including leukemia. Complex therapy is used in the treatment of Acute lymphoblastic leukemia (ALL) [50–55]: Doxorubicin, Vincristine, Methotrexate, Glucocorticoid (prednisone or dexamethasone), in combination with L-asparaginase enzyme-therapy. Treatment protocols include combinations of different drugs at each stage to minimize the risk of drug resistance and increase the likelihood of cure. Therefore, micellar formulations of Dox in combination, with L-asparaginase, represent promising ways to treat leukemia.

For a comprehensive study of smart drug delivery systems, we studied two fundamentally different types of cells: leukemia cells K562 and Raji lymphoma cells (i.e. blood cells with

 doi:10.20944/preprints202402.0157.v1

phagocytotic activity, presumably they will well absorb micellar particles with Dox) in comparison with skin cancer cells A875 (as a control type, non-phagocytic epithelial cells). In this way we could compare the permeability of different types of cells for Dox, non-covalent and covalent micellar formulations based on chitosan or heparin and correlate with antitumor activity. In this paper, the key idea is to increase the effectiveness and selectivity of the cytostatic drug taking advantage of the differences in morphology and metabolism of tumor cells against themselves, i.e. via implementing so called "aikido principle" by using the "smart" polymer nanoparticles. Thus, the creation of the drug carrier stable in blood circulation and disintegrate after intracellular uptake by tumor cells.

2. Results and Discussion

2.1. The synthesis and Characterization of Amphiphilic Polymers and Dox-Containing Micelles

2.1.1. Heparin and Chitosan Micelles

The concept is based on targeted delivery to tumors of the drug loaded in polymeric micelles. Tumor targeting is realized due to the pH-, thermo- (we shown earlier [31]) and glutathione-sensitivity of the micelles based on heparin and chitosan grafted with fatty acids (oleic and lipoic). We suggested polymeric micelles as drug delivery systems due to their dual nature: 1) the ability to incorporate drug molecules into the hydrophobic core, thereby solubilizing drug and protecting it from destruction, as well as drug ingestion into non-target cells and tissues; 2) Biocompatible polymers are harmless to the body and at the same time heparin has antithrombotic properties (thrombosis is increased in tumors) [42], chitosan has pH-sensitivity due to protonation of amino groups in a weakly acidic medium corresponding to the microenvironment of tumors.

To create an optimal delivery system, we studied both cationic and anionic polymers, as well as covalent and non-covalent micellar formulations with Dox. Table 1 shows the designations and characteristics of the developed polymers and micelles.

Table 1. Designations and characteristics of polymers and Dox-containing formulations based on polymeric micelles.

Dox containing micellar formulation		Dox mass percentage, %	Average Mw of one polymeric structure unit, kDa	Ref	
Brief designation*	**Chemical composition** ***			**Synthesis**	**FTIR spectra**
DoxM1	Dox in Chit5-LA	13±1	6.2±0.4	Figure 1a	Figures S1 and 3a
DoxM2	Dox in Chit5-OA	10±1	6.6±0.5		Figures 2a and 3a
DoxM3	Dox in Hep-OA	5.8±0.3	23±5		Figures 2b and 3a
DoxMC1	Dox-GSSG-Chit5-OA	13±1	8.3±0.7	Figure 1b,c	Figure 3b,c
DoxMC2	Dox-SS-LA-Chit5	14±1	7.5±0.6	Figure 1b,d	Figure 3b,d

* M means micellar, MC means micellar covalent. ** Chit5 – chitosan 5 kDa, Hep – heparin 20 kDa, LA – lipoic acid residue, OA – oleic acid residue, GSSG – reduced glutathione residue.

2.1.2. The Synthesis of Amphiphilic Polymers and Dox Prodrugs

To obtain micelles, firstly, amphiphilic polymers based on polycations or polyanions and hydrophobic substituents were synthesized. The schemes for chitosan and heparin grafted with fatty acids is shown in Figure 1a. The idea of synthesis is the activation of the carboxyl group of lipoic or

 doi:10.20944/preprints202402.0157.v1

oleic acids with subsequent crosslinking with the chitosan amino group using a carbodiimide approach. In the case of heparin, the situation is the opposite: the carboxyl group of heparin and the amino group of oleylamine are cross-linked using the same approach.

Obtaining covalent prodrugs based on Dox is a more cunning way. It is worth considering here that it is necessary to obtain not just a covalent crosslinking of the Dox-polymer, but a labile bond with the possibility of destruction only in the tumor microenvironment – this is a disulfide bond. Here we obtained the Dox-glutathione conjugate (Dox-GSSG, Figure 1b), which was used for subsequent obtaining of prodrugs (Figure 1c,d). DoxMC1: doxorubicin is attached to the polymer through cross-linked glutathione residues with S-S bond. DoxMC2: doxorubicin is attached to the polymer through glutathione residue and lipoic acid stitched with S-S bond.

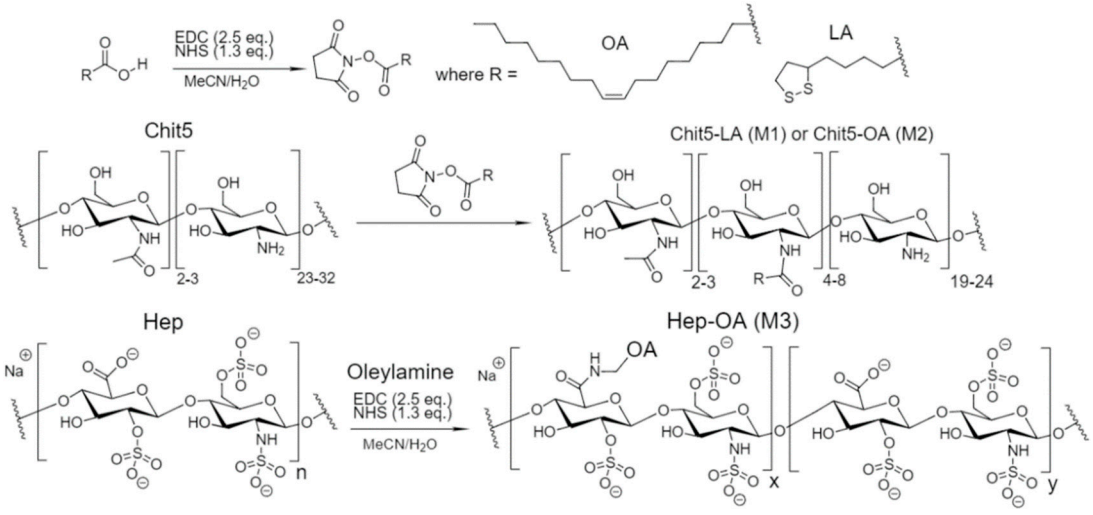

(**a**)

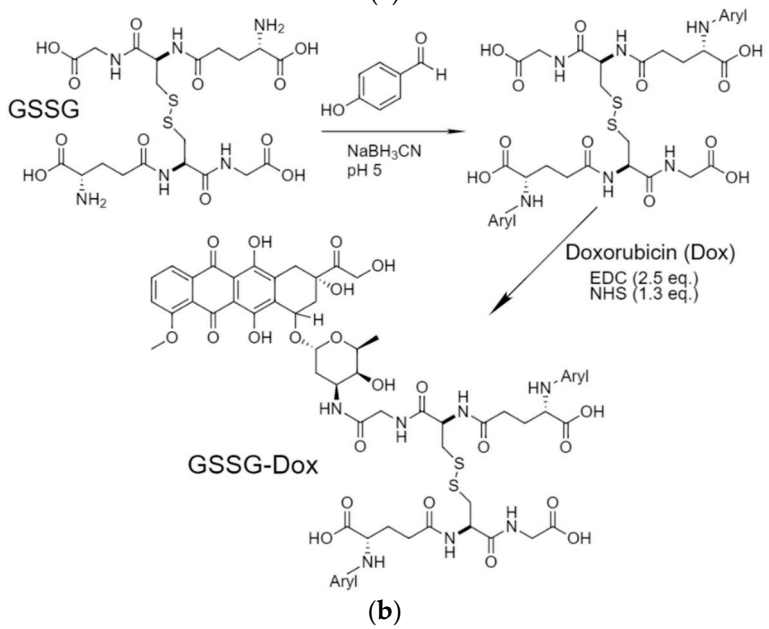

(**b**)

 doi:10.20944/preprints202402.0157.v1

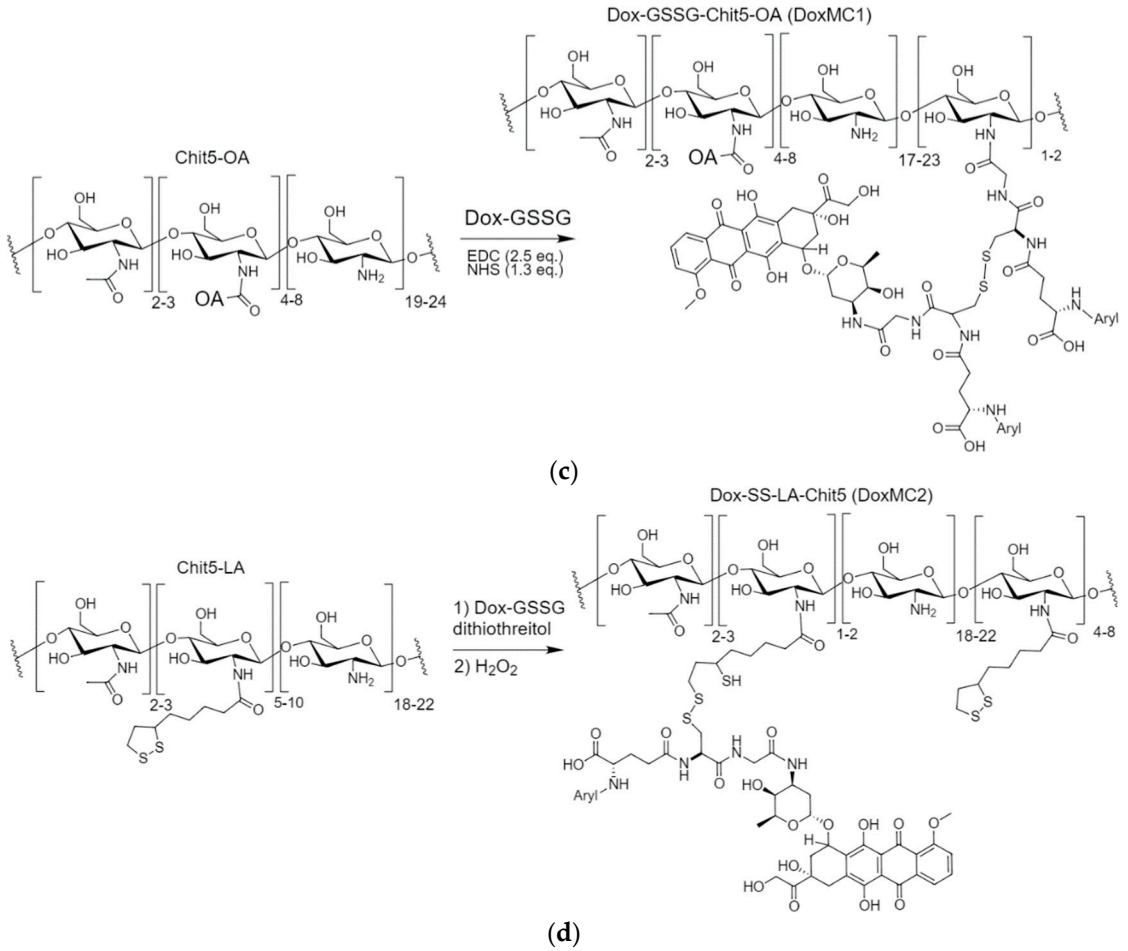

Figure 1. The schemes of synthesis of: (**a**) amphiphilic conjugates Chit5-LA, Chit5-OA and Hep-OA; (**b**) glutathione-sensitive doxorubicin **Dox-GSSG**; (**c**) covalent Dox conjugate Dox-GSSG-Chit5-OA (**Dox MC1**); (**d**) covalent Dox conjugate Dox-SS-LA-Chit5 (**Dox MC2**).

2.1.3. FTIR Spectroscopy for Characterization of Self-Assembled Chitosan and Heparin Conjugates

FTIR spectroscopy is one of the key methods for analyzing the molecular architecture and chemical structure of biological polymers, since such systems are complex and heterogeneous, which complicates the analysis by other classical methods such as mass spectrometry and NMR (are given in Supplement) spectroscopy. On the contrary, the IR spectra of biopolymers and conjugates are quite complaint to analysis and provide valuable information. Figure 2 shows FTIR spectra of chitosan (Chit5), oleic acid (OA), and Chit5-OA and Hep-OA conjugates. The spectra of OA and conjugates contains characteristic bands of valence oscillations of CH_2 groups in oleic residues (2980-2850 cm^{-1}). When chitosan is modified by oleic acid residues, the formation of an amide group C(=O)NH occurs from carboxylic group COOH, respectively, the intensity of the peak at 1710 cm^{-1} decreased, and two peaks appear at 1660 and 1560 cm^{-1} (Figure 2a). A part of chitosan amino groups modified into an amide crosslinking, therefore, the intensity of the NH oscillation band 3600-3200 cm^{-1} decreased. The grafting of chitosan with fatty acids leads to a change in the shape and structure of the peak of C–O–C bond oscillations (1200-1000 cm^{-1}) in the chitosan polymer chain: the two-component peak became multicomponent due to the different hydrophobicity of the microenvironment of glucosamine residues.

In the FTIR spectra (Figure 2b) of heparin (Hep) and its conjugate with oleylamine, high-intensity bands corresponding to sulfogroups (1250 cm^{-1}), as well as C–O–C oscillation band (1100-1000 cm^{-1}) are observed. Modification of heparin occurs due to the formation of an amide bond C(=O)NH, which is reflected in the IR spectra: two peaks appear at 1660 cm^{-1} (valence C=O) and 1560 cm^{-1} (deformational N–H) (Figure 2b). In addition, a peak corresponding to the valence oscillationы of N–H in the amide bond appears in the spectrum of the Нeз-OA conjugate compared to the Hep

 doi:10.20944/preprints202402.0157.v1

spectrum. Thus, FTIR spectroscopy confirms the chemical composition of amphiphilic polymers based on chitosan and heparin.

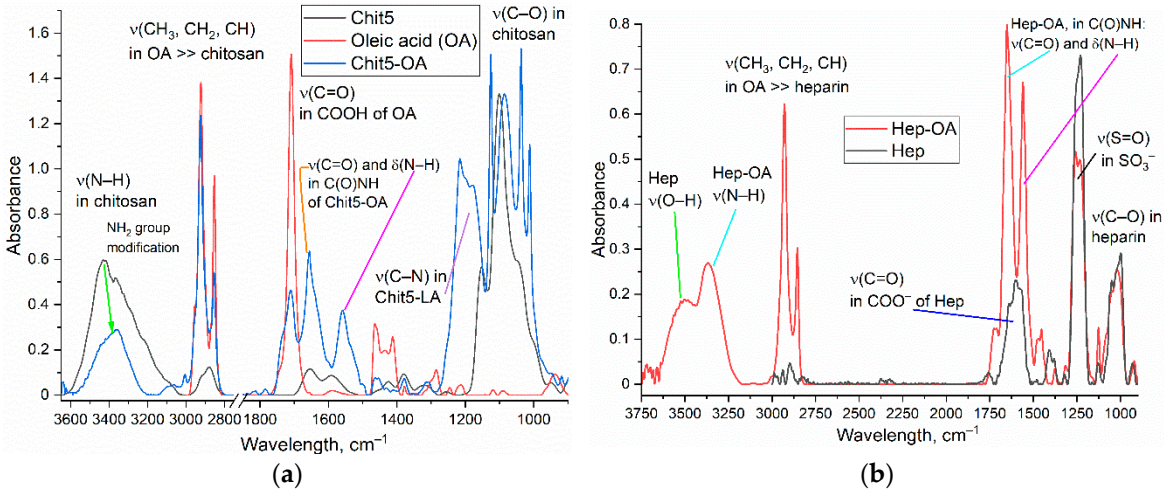

Figure 2. FTIR spectra of (**a**) Chit5, OA, its conjugate Chit5-OA; (**b**) Hep, Hep-OA. PBS (0.01 M, pH 7.4). T = 22 °C.

2.1.4. FTIR Spectroscopy for Characterization of Dox-Containing Micellar Formulations

The main objective of the work is to obtain cytostatic micellar formulations selective for tumors. An important parameter for the realization of selectivity is pH and glutathione sensitivity. The first is realized due to chitosan, the second due to disulfide bonds between polymer chains of amphiphilic conjugates in the micelle (polymer-polymer) or disulfide bonds Dox-polymer. These are two fundamentally different strategies for glutathione sensitivity, since covalent modification of the drug on the one hand will increase the target bioavailability, but at the same time may reduce the activity of the drug. Therefore, it is advisable to study both non-covalent micellar formulations based on Dox (*DoxM* series) and covalent Dox-polymer formulations (*DoxMC* series).

DoxM series. The FTIR spectra of Dox and non-covalent DoxM1-M3 formulations are shown in Figure 3a. All characteristic peaks of Dox are present in the spectra of micellar formulations: 1725 cm^{-1} (ν(C=O)), 1611 and 1582 cm^{-1} (δ(N–H)), 1445 and 1414 cm^{-1} (ν(C=C)), 1015 and 988 cm^{-1} (ν(C–O)). The inclusion degree of Dox in chitosan micelles (M1-M2) is about 10-13%, in heparin micelles is about 6% (Table 1). The inclusion of Dox in micelles is additionally confirmed by the shifts of the peak maximum in the IR spectra: 1) the peak at 1414 cm^{-1} shifts to 1411-1412 cm^{-1}, which indicates an increase in the hydrophobicity of the microenvironment of the aromatic Dox system in the core of micelles, 2) the peak of the carbonyl group oscillations shifts from 1724 to 1718-1721 cm^{-1}, which indicates a decrease in the hydration degree of the C=O group, that is an increase in the hydrophobicity of the microenvironment of the cytostatic molecule.

DoxMC series. The FTIR spectra of Dox and covalent polymeric formulations are shown in Figure 3b-d. In the FTIR spectrum of the conjugate of Dox and glutathione (GSSG) (Figure 3b), bands at 1640 and 1580 cm^{-1} appear corresponding to oscillations in the formed amide bonds of Dox-C(=O)NH-GSSG, as well as characteristic bands of both components. The synthesized Dox-GSSG conjugate was covalently attached via an amide bond to the Chit5-OA polymer (Figure 3c), and using thiol-disulfide exchange agents was attached via a labile S-S bond to lipoic acid residue in Chit5-LA polymer (Figure 3d, S2). The success of the synthesis is confirmed by the FTIR spectra in a similar way to the above reasoning: by the presence of peaks of all components and the appearance of peaks amide 1 and amide 2 after crosslinking. However, there are individual features for DoxMC1 and DoxMC2 conjugates. The formation of micelles from DoxMC1 polymers was accompanied by the formation of a hydrophobic core and the compaction of $(CH_2)_n$ tails (Figure 3c), while hydrophilic NH_2, OH groups are exposed outward into the water. For DoxMC2-based Dox-containing micelles, the key parameter is the presence of labile S-S bonds, which is confirmed by a decrease in the peak

 doi:10.20944/preprints202402.0157.v1

intensity of the corresponding oscillations of the S-H groups (Figure S2 – 2580, 2495 cm^{-1}) due to crosslinking. Thus, we have successfully synthesized non-covalent micellar Dox-containing formulations and covalent Dox-polymer conjugates.

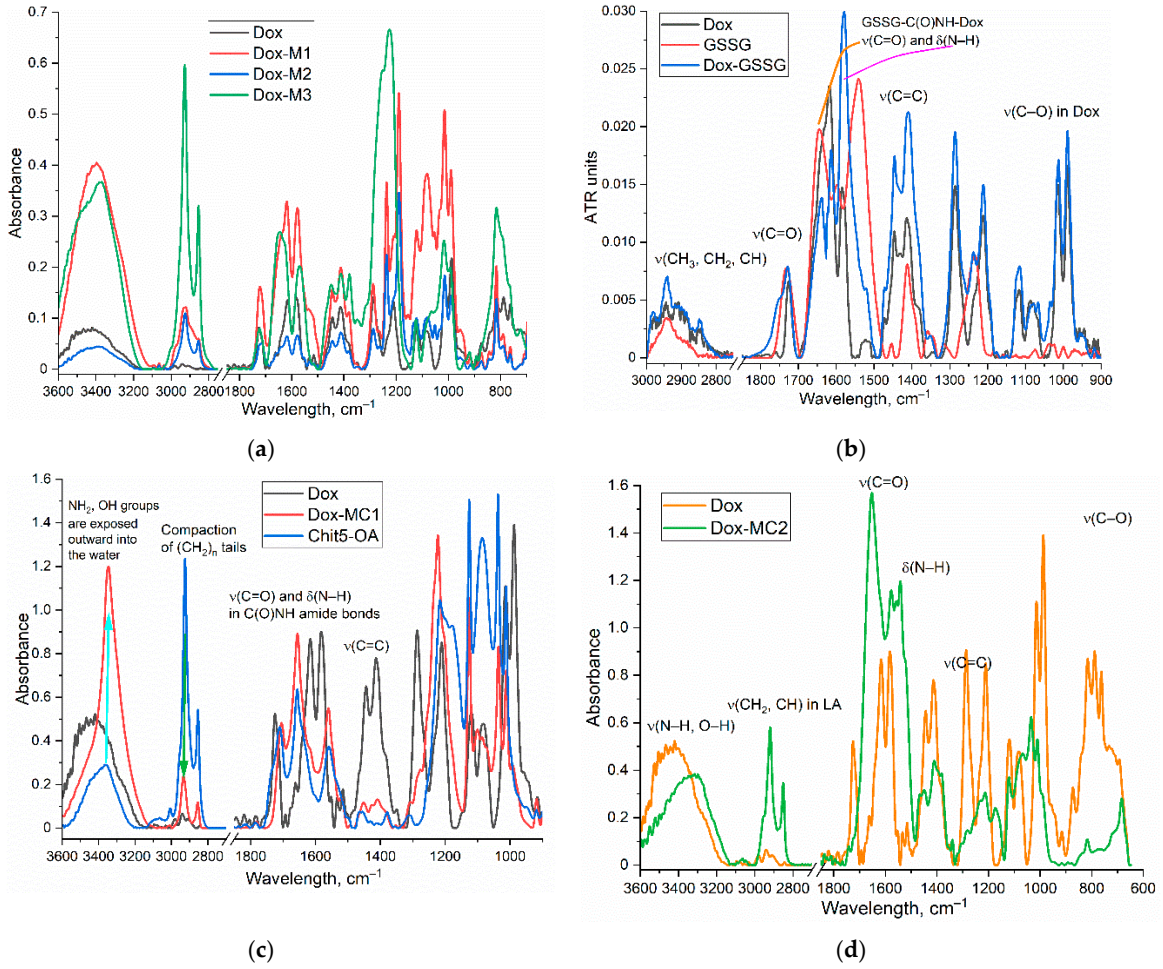

Figure 3. FTIR spectra of (**a**) Dox and its non-covalent micellar formulations Dox M1, M2, M3; (**b**) Dox, oxidized glutathione GSSG and its conjugate Dox-GSSG; (**c**) Dox and its covalent conjugate with Chit5-OA (Dox MC1); (**d**) Dox and its covalent conjugate with Chit5-LA (Dox MC2). PBS (0.01 M, pH 7.4). T = 22 °C.

2.2. Glutathione-Sensitivity of Conjugates

A key parameter for selective drug delivery to tumors is stimulus-sensitivity to the tumor cells microenvironment. Stimuli can be understood as 1) a slightly acidic environment (pH 5.5-6.5), 2) a local increase in temperature, 3) an increase in blood viscosity (thrombosis), 4) increased concentrations of reduced glutathione GSH. We examined the sensitivity of chitosan micelles to pH and temperature in a separate paper [31] and showed that: 1) at pH 5.5-6 (tumor microenvironment model), the rate of Dox release is 2–3 times higher than at pH 7-7.4; 2) Dox release rate was increased up to 2 times with a temperature increase from the physiologically relevant 37 °C to local inflammatory zone with 42 °C. We investigated the third aspect regarding antithrombotic drug delivery systems to tumors, since we developed the heparin based polymeric micelles, since heparin is an antithrombin activator [43–46].

And finally, the most important aspect is glutathione sensitivity, that is, the ability of micelles to release the drug at elevated GSH concentrations (up to 20 mM). At the same time, the difference in the concentration of glutathione (GSH) inside cells (2-4 mM, in tumor cells 4-5 times higher to 20-30 mM) and in extracellular fluid (2-20 μM). We have developed non-covalent micellar formulations with Dox (DoxM1-M3), which significantly slow down the rate of Dox release (Figure 4, Table 2)

 doi:10.20944/preprints202402.0157.v1

compared with free drug, however, the nature of this release is not glutathione-dependent. At the same time, covalent conjugates DoxMC1 and DoxMC2 demonstrate an increase in the initial rate of Dox release up to 6 times in the presence of 10 mM GSH, while in 7 h the accumulated concentration of Dox is 5-6 times higher in the model tumor microenvironment. Thus, the covalent conjugates DoxMC1-MC2 are glutathione-sensitive and able to selectively release the drug in the tumor microenvironment.

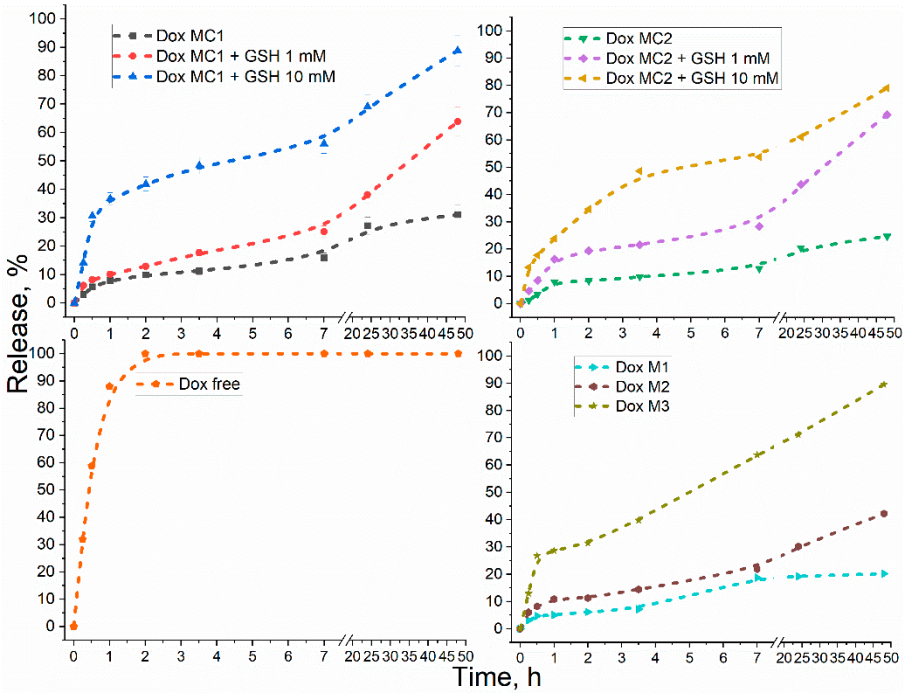

Figure 4. Dox release kinetic curves for different formulations; Dox free, Dox non-covalent micellar formulations and Dox covalent conjugates in presence of 0/1/10 mM reduced glutathione (GSH). PBS (0.01 M, pH 7.4). T = 37 °C. DoxM1 – Dox in Chit5-LA, DoxM2 – Dox in Chit5-OA, DoxM3 – Dox in Hep-OA, DoxMC1 – Dox-GSSG-Chit5-OA, DoxMC2 – Dox-SS-LA-Chit5.

Table 2. Kinetic parameters of Dox release: initial rates, accumulated release concentrations after 7 hours. Dialysis method in an external solution (1 to 10 by volume, membrane with a cut-off mass of 7 kDa). C_{Dox} = 1 mg/mL. PBS (0.01 M, pH 7.4). T = 37 °C. For Dox free and Dox M1-M3, the release rate was practically independent of the GSH concentration (no more than 10%).

Dox formulation	Initial rate, %/h	Accumulated concentration after 7 h, %
Dox free	88±5	100
DoxM1	5±1	19±2
DoxM2	11±2	22±3
DoxM3	29±4	64±5
DoxMC1	8±1 (0 mM GSH) 10±1 (1 mM GSH) 37±4 (10 mM GSH)	16±3 (0 mM GSH) 25±4 (1 mM GSH) 64±7 (10 mM GSH)
DoxMC2	8±1 (0 mM GSH) 16±2 (1 mM GSH) 25±2 (10 mM GSH)	13±2 (0 mM GSH) 28±3 (1 mM GSH) 54±5 (10 mM GSH)

2.3. Cytotoxicity Studies of Drugs

Table 3 shows the data of MTT analysis of model leukemic cancer cell K562 viability after 1 and 3 days of incubation with Dox-containing formulations. Free Dox works confidently, however, its effect on cells limits the survival rate to 30%, which is insufficiently effective. At the same time,

 doi:10.20944/preprints202402.0157.v1

micellar non-covalent formations DoxM1-M3 demonstrate the dose-dependent nature of cytostatic activity and, at a concentration of 50 μM, reduce cell viability to 14% on the first day. It is worth considering that the drug releases from the non-covalent micelles for hours-days (Figure 4), therefore, the powerful effect of micellar cytostatics is achieved mainly on day 3: cell viability is close to 0. In the case of covalent conjugates, reduced activity (compared to free Dox) is observed on day 1 due to covalent crosslinking with the polymer and consequently reduced permeability to cells.

The cytostatic effect of conjugates strongly depends on the incubation time when Dox is released due to glutathione in cancer cells microenvironment – proof of selective action only in tumors. Covalent conjugates on day 3 revealed their potential and would demonstrate true selectivity to tumors (if the Dox was not released, there would be no cytostatic effect). The indifference of S-S cross-linked micelles was observed in relation to the model of normal HEK293T cells, since pH 7.4 is maintained in the medium of normal cells, and there is no excessive amount of glutathione – there is no trigger for micelles. Indeed, the action of the covalent conjugates on normal HEK293T cells was significantly reduced compared to free drug (Figure S3).

Table 3. K562 cells viability MTT assay. Cells were treated with Dox-containing formulation: 5 and 50 μM. RPMI-1640 medium supplemented with 5% fetal bovine serum and 1% sodium pyruvate at 5% CO_2/95% air in a humidified atmosphere at 37 °C. DoxM1 – Dox in Chit5-LA, DoxM2 – Dox in Chit5-OA, DoxM3 – Dox in Hep-OA, DoxMC1 – Dox-GSSG-Chit5-OA, DoxMC2 – Dox-SS-LA-Chit5.

Dox formulation	C_{Dox} = 50 μM		C_{Dox} = 5 μM	
	1 day	3 day	1 day	3 day
Dox free	30±3	4.3±0.5	33±2	5±1
Dox M1	31±2	< 1	43±4	3.3±0.3
Dox M2	26±3		40±5	4.1±0.7
Dox M3	14±1		23±1	2.9±0.2
Dox MC1	54±5	6.4±1.2	69±8	29±5
Dox MC2	57±8	5.3±1.1	81±6	21±3

2.4. Permeability of Raji Cancer Cells to Dox-Containing Formulations

We have shown an improved cytostatic effect of micellar formulations of Dox, as well as selectivity to tumors cells of covalent conjugates. To confirm the observed effects, we conducted a kinetic experiment (Figure 5a) to determine the permeability of Dox formulations in lymphoma cancer cells Raji. The data are given regarding the kinetics of free Dox – for convenience of interpretation: the increasing course of the curves relative to the control (free Dox) indicates the Dox release from the micelles, followed by penetration into cancer cells. Micellar formulations (DoxM1 – Dox in Chit5-LA, DoxM2 – Dox in Chit5-OA, DoxM3 – Dox in Hep-OA) actively release Dox (in the presence of cells), and covalent conjugates (DoxMC1 – Dox-GSSG-Chit5-OA, DoxMC2 – Dox-SS-LA-Chit5) rather slowly, which is consistent with the data on Dox release in the presence of glutathione in the absence of the cells (Figure 4). Comparing systems with and without cells, the growth of the fluorescence signal increases to a quarter of the initial one, which indicates Dox penetration into cells and ignition of fluorescence. There are interesting observations for covalent conjugates (containing -S-S- bonds): in the absence of cells, Dox detachment does not occur (the curves slightly differ from the Dox free control), while in the presence of cancer cells, an increasing course of curves is observed, which indicates to Dox release and its gradual accumulation in Raji cells. Thus, we have shown the effectiveness of micellar conjugates against tumor cells. An interesting effect has been revealed – the ability to observe the release of drugs from micelles and penetration into cells using fluorimetry without using microscopy, while the data are well correlated. An important observation can be made by comparing heparin and chitosan micelles (green and red curves): in the presence of cells, a noticeable difference is observed for chitosan-based DoxM1-2 micelles, while in the case of heparin DoxM3 micelles, the difference is not so pronounced. This fact can be explained by the values of the zeta potentials of cells and polymers: ζ-potential of human cells at pH 7.5 are approximately –20 mV, heparin micelles – –45-30 mV, chitosan micelles - about +20-30 mV. Therefore, chitosan micelles are

 doi:10.20944/preprints202402.0157.v1

more actively adsorbed on the surface of cancer cells. In addition, in the presence of cells, stimulus–sensitive of covalent Dox-containing conjugates are realized – significant change in lilac curve was observed due to sensitivity to the tumor microenvironment.

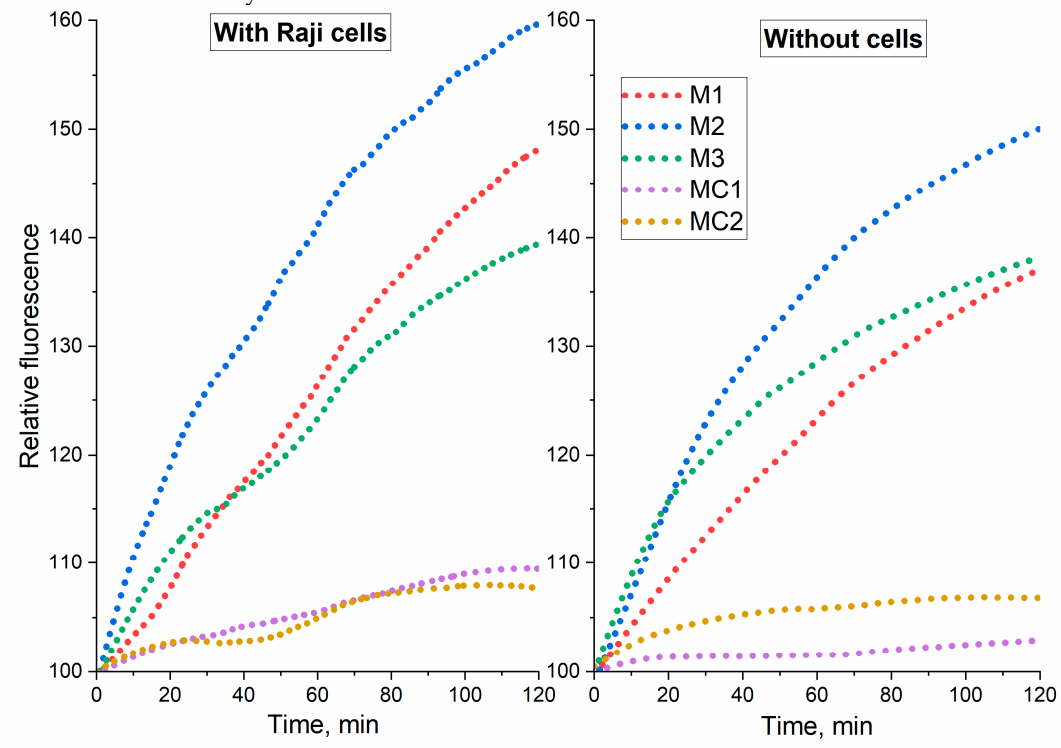

(**a**)

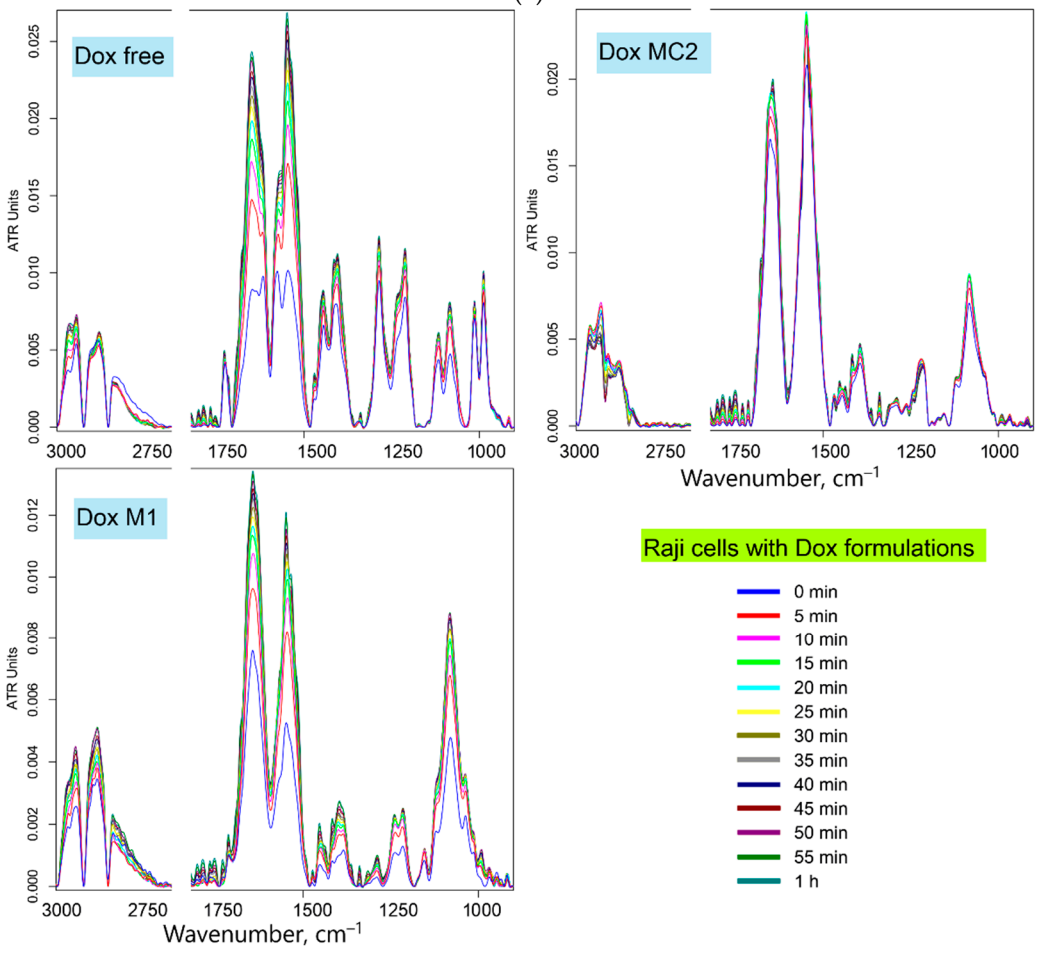

(**b**)

 doi:10.20944/preprints202402.0157.v1

Figure 5. (**a**) Kinetic curves of the relative fluorescence compared to the control free Dox (sample fluorescence / free Dox fluorescence) during incubation of Dox-containing (20 μM) formulations in buffer solution and in the presence of Raji cells (10^6 cells/mL). PBS (0.01 M, pH 7.4). T = 37 °C. λexci = 480 nm. λemi = 590 nm. (**b**) FTIR spectra of Raji cells (10^7 cells/mL) during incubation with Dox-containing formulations. PBS (0.01 M, pH 7.4). T = 37 °C. DoxM1 – Dox in Chit5-LA, DoxM2 – Dox in Chit5-OA, DoxM3 – Dox in Hep-OA, DoxMC1 – Dox-GSSG-Chit5-OA, DoxMC2 – Dox-SS-LA-Chit5.

2.5. Dox-Containing Formulation Interactions with Eukaryotic Cells: The Molecular Details

We have shown an improved cytostatic effect of micellar formulations of Dox, as well as selectivity Regarding the cells permeability for the drug formulations, we have recently developed obvious and sensitive technique based on FTIR spectroscopy [56], providing complementary information regarding the details of the drug's interaction with individual cell components. Here, to clarify the molecular details of the interactions of Dox and its micellar forms with cancer cells (Raji), we used FTIR spectroscopy (Figure 5b). Characteristic peaks corresponding to oscillations in the bonds of the components of the lipid bilayer (3000-2850 cm^{-1}), proteins (amide I 1700-1600 cm^{-1}, amide II 1600-1500 cm^{-1}), carbohydrate fragments (1100-1000 cm^{-1}) appear in the FTIR spectra of cells. The penetration of Dox into cells is accompanied by an increase in peak intensity: amide I is analytically significant. In the case of free Dox, there is a 2.5-fold increase in the intensity of amide I per hour, in the case of micellar non-covalent Dox there is a 2-fold increase and small 15-20% change for the covalent conjugate, which is consistent with the data in Figure 5a. The interaction of micelles with the cell membrane is accompanied by an increase in peak intensity at 1100-1000 cm^{-1}. The greatest change is observed in the case of the non-covalent micellar (only in this combination) formation of DoxM1, since the structure of non-crosslinked micelles is looser than covalent linked. However, Dox in chitosan micelles intercalates more effectively into DNA (band 1300-1200 cm-1) than in the case of a simple dox. At the same time, if the drug weakly penetrates and interacts (as in the case of covalent micelles DoxMC1-2), then small changes are observed – control of the validity of the method. Thus, using FTIR spectroscopy, we have shown that non-covalent micellar Dox penetrates cancer cells efficiently, and the cleavage of Dox from the covalent conjugate is slowed, but necessary for prolongation and selectivity.

To prove the selectivity of the action of micelles on eukaryotic cells, the authors used normal HEK293T cells as a control (Figure S3). At 37 °C Dox effectively penetrates cells (we observe an almost 3-fold increase in the intensity of amide I), while micellar DoxM1 penetrates much weaker (less than 10% of the change in spectra). thus, micellar formations show selectivity to cancer cells.

2.6. Confocal Visualization of Micellar Formulations Based on Doxorubicin Action on Cancer Cells

One of the highly informative methods for visualizing the effect of cytostatics on cells is confocal laser scanning microscopy (CLSM). Figures 6ab show fluorescent images of cells A875 and K562 incubated with Dox formulations: micellar non-covalent Dox, micellar covalent Dox in comparison with free Dox. In the case of A875 cells, the best permeability is achieved for DoxM1, while covalent doxorubicin penetrates relatively weakly (during the incubation time of 2 hours). In contrary, in the case of the leukemia cell K562, we observe high efficiency of both micellar formulations and the covalent conjugate of Dox, which demonstrated the highest efficiency. The accumulation of Dox in the nucleus of cancer cells is a characteristic feature of this cytostatics, and this is observed of in the case of free Dox and covalent conjugate DoxMC1 (purple and blue colors in the Merge channel). On the contrary, non-covalent micellar DoxM1, due to its high adsorption on the cell surface, causes a predominantly purple color (wider area coverage) in the Merge channel (zoom in Figure 6a)

Figure 7 shows confocal images of Raji cells pre-incubated with all the studied formulations. The greatest efficiency of Dox penetration into cancer cells is achieved in the case of micellar formulations: covalent (DoxMC1-2) or heparin-based (DoxM3). Taking into account the prolonged release of Dox, this is a significant result. That is, in the case of micellar cytostatics, the bioavailability of the drug is significantly higher, while penetration into healthy cells is reduced, as we have shown earlier [31].

 doi:10.20944/preprints202402.0157.v1

Quantitative data on the permeability of Dox-containing formulations are presented in Figure 8. Heparin micelles with Dox (DoxM3, which showed also better activity according to the MTT test), as well as covalent conjugates (DoxMC1-2), penetrate most actively. At the same time, it is worth noting that incubation was carried out for 2 hours (conditions to identify differences between the formulations), therefore covalent DoxMC1-2 has not yet revealed its potential, which could be realized after 48-72 h. Micrographs of Raji and K562 cells show that almost all of the Dox-containing samples were completely absorbed. Absorption occurs partially with polymeric particles since their size is 200-250 nm – internalization into phagocytic Raji and K562 cells. This means that the effectiveness of cytostatic accumulation in the tumor is retained, and selectivity will be ensured compared to healthy cells.

At the same time, on the example of skin A875 cells, the penetration of polymeric particles is noticeably much less, since they are surface attached and non-phagocytic. The resulting efficiency for the studied samples is shown in Table 4.

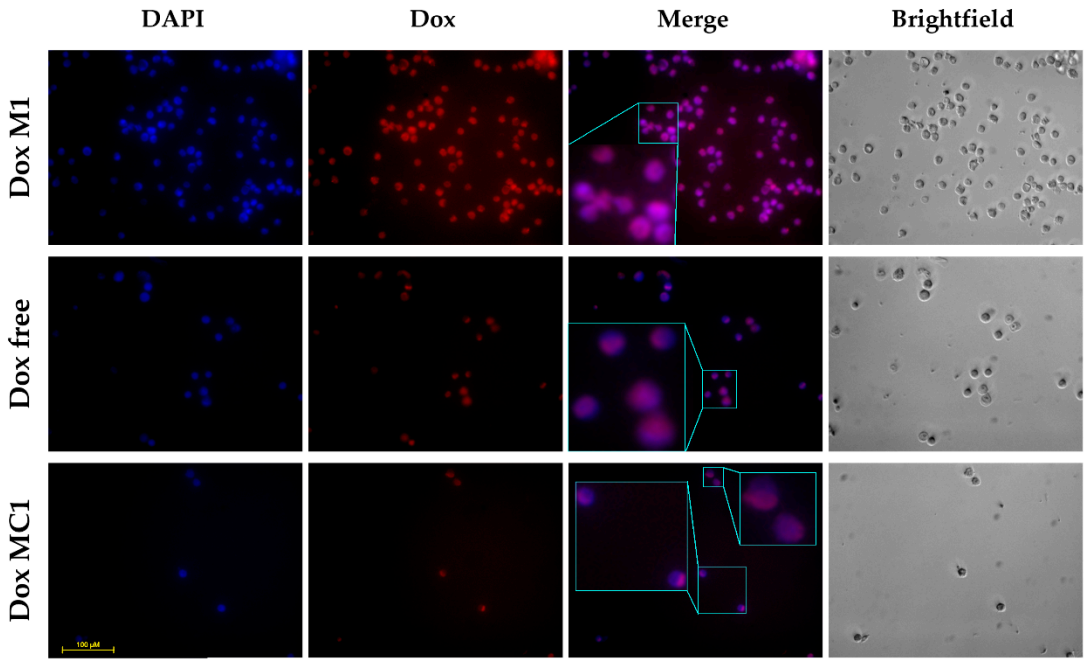

(**a**)

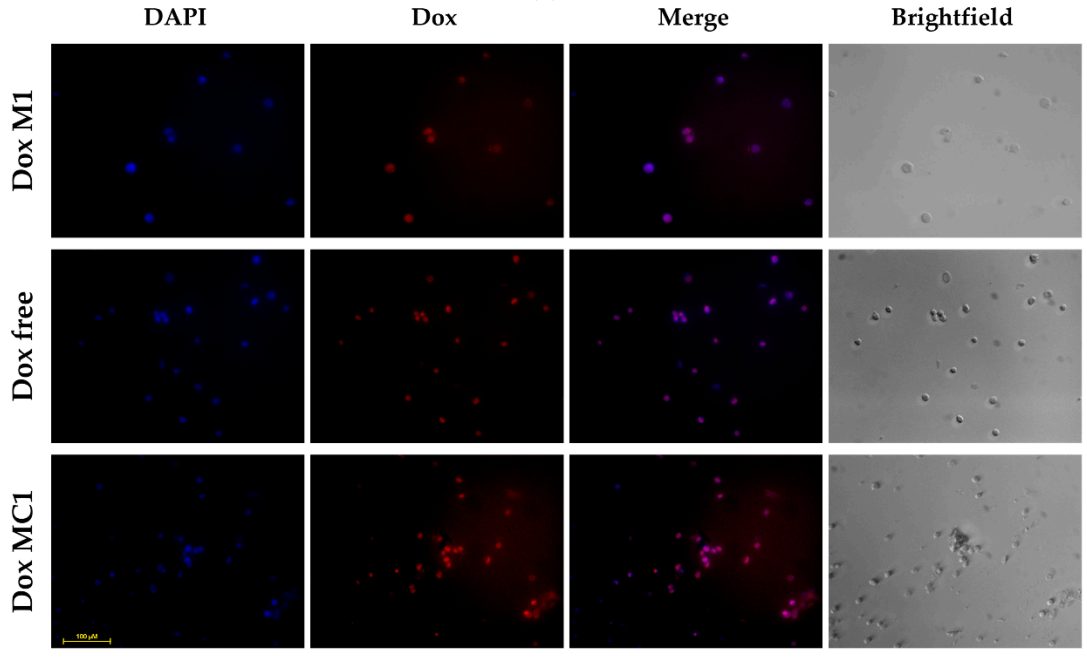

(**b**)

 doi:10.20944/preprints202402.0157.v1

Figure 6. Fluorescence images of (a) A875 cells, and (b) K562 cells after 2 h incubation with Dox-containing formulations. C_{Dox} = 2 μM. The nuclei are stained with DAPI (1 μg/mL). DAPI channel: λ_{exci} = 310-380 nm, λ_{emi} = 420-500 nm. Dox channel: λ_{exci} = 500–560 nm, λ_{exci} = 590-700 nm. The scale segment is 100 μm. DoxM1 – Dox in Chit5-LA, DoxM2 – Dox in Chit5-OA, DoxM3 – Dox in Hep-OA, DoxMC1 – Dox-GSSG-Chit5-OA, DoxMC2 – Dox-SS-LA-Chit5.

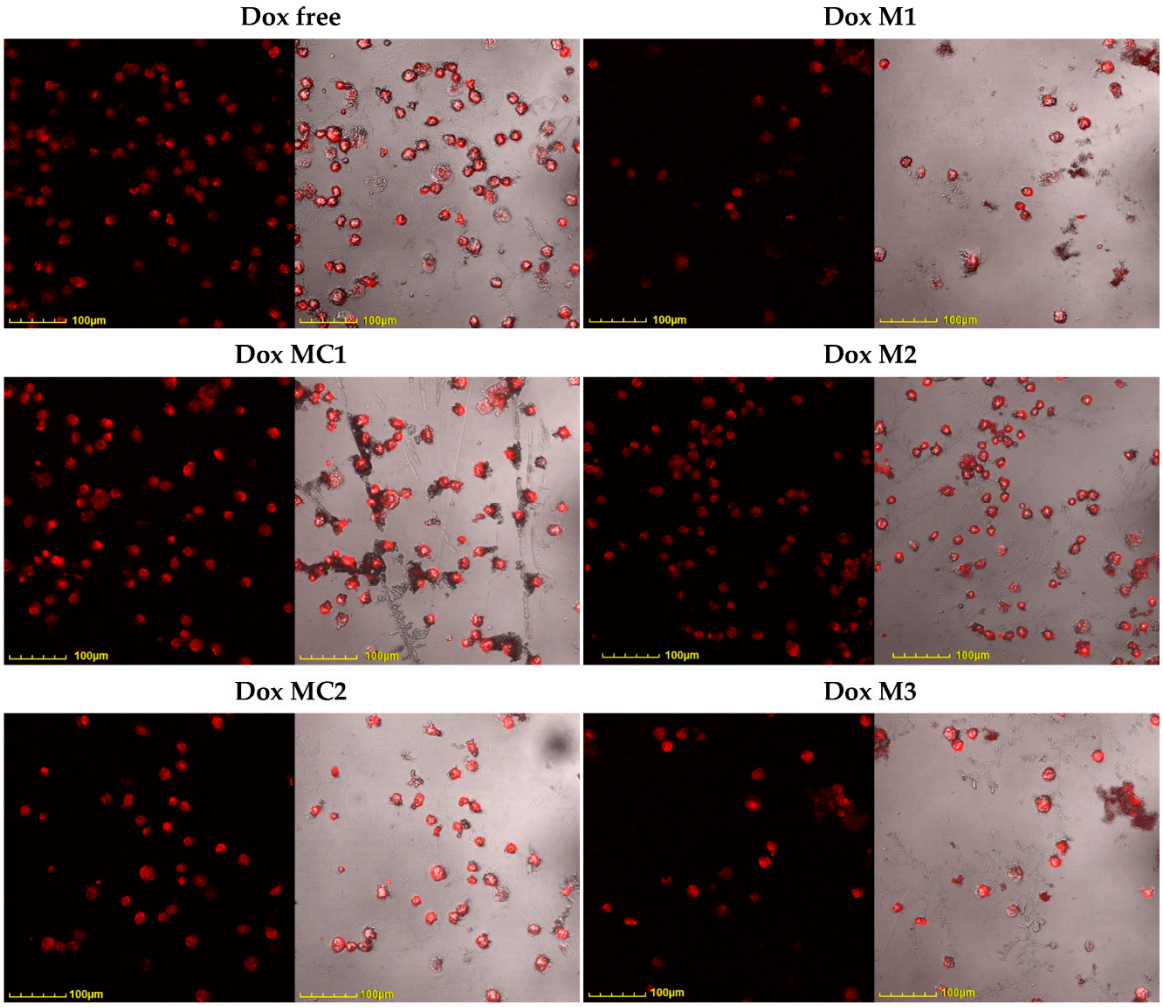

Figure 7. Confocal laser scanning fluorescence images of Raji cells after 2 h incubation with Dox-containing formulations. C_{Dox} = 10 μg/mL. λ_{exci} = 488 nm, λ_{emi} = 570-730 nm. The scale segment is 100 μm. DoxM1 – Dox in Chit5-LA, DoxM2 – Dox in Chit5-OA, DoxM3 – Dox in Hep-OA, DoxMC1 – Dox-GSSG-Chit5-OA, DoxMC2 – Dox-SS-LA-Chit5.

 doi:10.20944/preprints202402.0157.v1

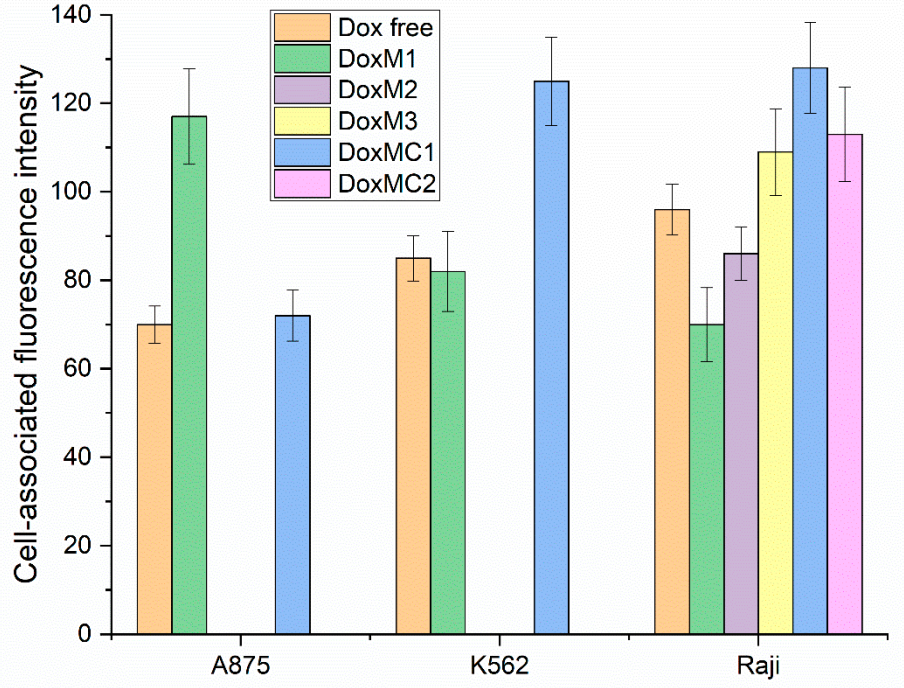

Figure 8. Cell-associated Dox fluorescence values depending on the composition of the Dox-containing formulation (10 μg/mL). Determined by fluorescent image analysis and fluorescence quantification of Dox uptake. PBS (0.01M, pH 7.4). T = 37 °C. DoxM1 – Dox in Chit5-LA, DoxM2 – Dox in Chit5-OA, DoxM3 – Dox in Hep-OA, DoxMC1 – Dox-GSSG-Chit5-OA, DoxMC2 – Dox-SS-LA-Chit5.

Table 4. The resulting schematic characteristics of Dox-containing formulations based on polymeric micelles in terms of tumor targeting. "++" means a bright effect, "+" means a good effect, "±" means a weak effect, "–+" means a very weak effect, "–" there is no effect.

Dox containing micellar formulation		Permeability to eukaryotic cells				Toxicity to eukaryotic cells		Tumor-sensitivity	
Brief designation	Chemical composition	Cancer K562	Cancer Raji	Cancer A875	Normal HEK293T	Cancer K562	Normal HEK293T	pH 5.5–6.5	glutathione
Dox	Dox free	+	+	±	+	+	+	–	–
DoxM1	Dox in Chit5-LA	++	±	+	±	++	±	+	+
DoxM2	Dox in Chit5-OA	+	+	+	±	++	±	+	–
DoxM3	Dox in Hep-OA	++	++	+	±	++	±	±	–
DoxMC1	Dox-GSSG-Chit5-OA	+	++	++	–	+	–+	+	++
DoxMC2	Dox-SS-LA-Chit5	+	++	+	–	+	–+	+	++

3. Conclusions

The paper considers an approach to the creation of the cytostatic drug carrier (Dox) stable in blood circulation and disintegrate after intracellular uptake in leukemic cells. Polymeric micelles

 doi:10.20944/preprints202402.0157.v1

based on chitosan, heparin and fatty acid residues (lipoic or oleic) are characterized by pH-, thermo- and glutathione sensitivity to the tumor microenvironment. In a weakly acidic environment, protonation of chitosan amino groups occurs, resulting in loosening of the micelle structure and release of the drug into cancer cells. We have obtained both non-covalent micellar formulations with doxorubicin (Dox) and covalent Dox-SS-polymer compounds in which the RedOx-sensitive disulfide bond is a trigger to the tumor environment. Using fluorescence and FTIR spectroscopy, we have shown the prolonged nature of the release of Dox from the nanoparticles. At the same time, it was found that the release rate increases up to 6 times in the presence of glutathione as a model substance in the tumor environment. For Dox-SS-polymer conjugates in the absence of cells Dox detachment does not occur, while in the presence of cancer cells Dox release and its gradual accumulation in Raji cells were observed – a direct indication of the stimuli-sensitivity of micelles. Using FTIR spectroscopy, the molecular details of the interaction of Dox-containing formulations with eukaryotic cells were determined and the selectivity of the action of micellar Dox against cancer cells Raji vs normal cells HEK293T was shown. Using confocal microscopy, the penetration of Dox-containing formulations into cancer cells of two types was visualized: phagocytic cells, capable to absorb large particles such as micelles – Raji and K562; and skin cancer cells A875 (epithelial, non-phagocytic cells), weakly absorbing large polymer particles. We regard the most optimal formulations for the treatment of leukemia: Dox in Hep-OA and Dox-GSSG-Chit5-OA. Chitosan micelles, both covalent and non-covalent, can be used to treat skin cancer. Enhanced metabolism of cancer cells and the tendency to absorb the large particles, tumors maintain high levels of glutathione and a slightly acidic environment, but at the same time this is the weak point. This was taken advantage when using "smart" stimuli-sensitive micelles – via implementing the "Aikido principle".

4. Materials and Methods

4.1. Reagents

In this work the following chemicals were used: chitosan 5 kDa (Chit5), heparin 20-30 kDa (Hep), oleic acid (OA), lipoic acid (LA), 1-Ethyl-3-(3-dimethylaminopropyl) carbodiimide (EDC), N-hydroxysuccinimide (NHS), doxorubicin (Dox) hydrochloride from Sigma Aldrich (St. Louis, MI, USA). Dithiothreitol, acid, solvents, salts and others were Reachim production (Russia, Moscow).

4.2. The Synthesis and Characterization of Amphiphilic Polymers and Dox-Containing Micelles

4.2.1. Heparin and Chitosan Grafted Conjugates Synthesis

Chit5-OA and **Chit5-LA**. The oleic acid (OA) and lipoic acid (LA) 30 mg were dissolved in 5 mL CH_3CN/PBS (4:1 v/v, pH 7.4). 2.5-fold molar excess of EDC and 1.3-fold molar excess of NHS were added in DMF. Acid activation was performed for 20 minutes at 50 °C. Then pre-dissolved Chit5 (90 mg in 10 mL 1 mM HCl, followed by pH adjustment to 7) was added to the reaction mixtures. Then the mixtures were incubated for 6 hours at 50 °C. The reaction mixtures were purified using centrifuge filters (3 kDa, 10,000 g, 3×10 min), then dialyzed against water for 12 h (cut-off 6-8 kDa). Chit5 modification degree was estimated from spectrophotometric titration technique using 2,4,6-trinitrobenzenesulfonic acid in sodium-borate buffer (pH 9.2).

Hep-OA. 125 mg of heparin (Hep) was dissolved in 10 mL of PBS. 2.5-fold molar excess (in relation to the amount of oleylamine) of EDC and 1.3-fold molar excess (in relation to the amount of oleylamine) of NHS were added in DMF. Hep activation was performed for 20 minutes at 50 °C. Then pre-dissolved oleylamine (40 mg in 5 mL CH_3CN/PBS (4:1 v/v, pH 7.4)) was added to the reaction mixture followed by incubataion for 6 hours at 50 °C. The reaction mixtures were purified using centrifuge filters (10 kDa, 10,000 g, 3×10 min), then dialyzed water for 12 h (cut-off 12-14 kDa).

All samples were freeze-dried at –60 °C (Edwards 5, BOC Edwards, UK).

 doi:10.20944/preprints202402.0157.v1

4.2.2. Non-Covalent Dox Micellar Formulation Synthesis

DoxM1-M3. Chit5-LA, Chit5-OA and Hep-OA were dissolved in PBS (0.01M, pH 7.4) at concentration 10 mg/mL. Dox solution (2 mg/mL) was added to these solutions until the loading degrees indicated in Table 1 were reached ± 1%. Micelle samples were prepared by probe-type ultra-sonic treatment (snow, 10 min) followed extrusion through a 200 nm membrane.

4.2.3. Covalent Dox Micellar Formulation Synthesis

Dox-GSSG. Oxidized glutathione was incubated with 3-mol equivalents of 4-hydroxybenzaldehyde in the presence of 5 eq. $NaBH_3CN$ at pH 5 (sodium acetate buffer) for 2 hours at 60 °C. Then 1 mL of 3% H_2O_2 was added to the mixture. The mixture was purified using centrifuge filters (3 kDa, 10,000 g, 5 min). Dox was incubated for 3 h at 40 °C in PBS with protected GSSG (1:1.2 mol/mol) in the presence of 2.5-fold molar excess of EDC and 1.3-fold molar excess of NHS. Dox-GSSG was purified using dialysis against water for 12 h (cut-off 1 kDa).

DoxMC1 (Dox-GSSG-Chit5-OA). Chit5-OA was incubated for 4 h at 40 °C in PBS with Dox-GSSG (1:2 mol/mol) in the presence of 2.5-fold (on Dox) molar excess of EDC and 1.3-fold molar excess of NHS. Dox-GSSG-Chit5-OA was purified using dialysis against water for 12 h (cut-off 6-8 kDa).

DoxMC2 (Dox-SS-LA-Chit5). Chit5-LA was incubated for 2×30 min at 60 °C in PBS with Dox-GSSG (1:2 mol/mol) in the presence of: 1) 3-fold molar excess of dithiothreitol, 2) 10-fold molar excess of H_2O_2. Dox-SS-LA-Chit5 was purified using dialysis against water for 12 h (cut-off 6-8 kDa).

All samples were freeze-dried at –60 °C (Edwards 5, BOC Edwards, UK). Micelle samples were prepared by probe-type ultra-sonic treatment (snow, 10 min) followed extrusion through a 200 nm membrane.

4.3. Characterization of Polymers and Micelles

FTIR spectra of samples were registered using a FTIR microscope MICRAN-3 and Bruker Tensor 27 spectrometer equipped with a liquid-nitrogen-cooled MCT (mercury cadmium telluride) detector, as described earlier [31,57].

^1H spectra of samples were registered using a Bruker Avance 400 spectrometer (Bruker, Ettlingen, Germany) with an operating frequency of 400 MHz: Figure S4.

Circular dichroism spectra were recorded on Jasco J-815 CD Spectrometer (JASCO, Tokyo, Japan), and were used to estimate the deacetylation degree in Chit5, which amounted to (92±3)%.

Atomic force microscopy (AFM microscope NTEGRA II, NT-MDT Spectrum Instruments, Moscow, Russia) was used to visualize polymeric micelles based on grafted chitosan and compare it in terms of shape and size with non-modified chitosan. The size is ranged from 250 to 350 nm for chitosan micelles, and about 400-450 nm for heparin micelles.

4.4. Determination of Dox Loading Degree into Micelles and Release Kinetics

The amount of Dox loaded in micellar formulations was determined by absorption at 488 nm and fluorescence intensity at 590 nm.

The release experiment was structured as follows. 1 mL of the Dox-containing solution (1 mg/ml) was placed inside a dialysis bag with a cut-off weight of 7 kDa and then bag was placed in an external solution PBS (10 mL, 0.01M, pH 7.4). The system was incubated at 37 °C and samples were taken in which Dox was determined fluorimetrically.

UV-vis spectra of solutions were recorded on the AmerSham Biosciences UltraSpec 2100 pro device (Cambridge, UK). Fluorescence of Dox was measured using a Varian Cary Eclipse spectrofluorometer (Agilent Technologies, Santa Clara, CA, USA) at 22 °C: λ_{exci} = 490 nm, λ_{emi} = 560 nm.

 doi:10.20944/preprints202402.0157.v1

4.5. Cell Cultivation and Toxicity Assay

K562 leukemia cells, A875 melanoma cells, Raji lymphoblast-like cells, linear cells of the embryonic kidney human epithelium HEK293T were obtained from Lomonosov Moscow State University Depository of Live Systems Collection (Moscow, Russia). Cells were grown in RPMI-1640 medium (Gibco, Thermo Fisher Scientific Inc., Waltham, MA, USA) supplemented with 5% fetal bovine serum (Capricorn Scientific, Ebsdorfergrund, Germany) and 1% Na-pyruvate (Paneco, Moscow, Russia) at 5% CO_2/95% air in a humidified atmosphere at 37 °C.

4.6. FTIR Spectroscopy as A Tool for Studying of Dox Interaction with Cells

Cell suspension (3-5 ×10^6 cells/mL) were washed twice with sterile PBS (pH = 7.4) from the culture medium by centrifuging (Eppendorf centrifuge 5415C, 2×5 min, 4,000×g).

Cells were precipitated followed by resuspention in PBS to concentration 1×10^7 cells/mL. 20 uL of cell suspension was placed on a spectrometer chamber, 10 μl of Dox-containing preparation was added (1 mg/mL according to Dox), the samples were incubated at 37 °C and spectra were recorded in increments of 5-10 min. Absorbed by cells and free Dox were quantified using fluorescence spectroscopy.

4.7. Confocal Laser Scanning Microscopy for Visualization of Dox Interaction with Cells

Cells were precipitated as described above followed by 2 h incubation with Dox-containing formulations (10 μg/mL on Dox). The cells were washed twice with PBS (5 min, 4,000×g) followed by placing in 96-well tablet cells and treating with formaldehyde. Confocal images were recorded on the confocal laser scanning microscope (CLSM) Olympus FluoView FV1000 equipped with both a spectral version scan unit with emission detectors and a transmitted light detector. The scan area was 80 × 80 μm^2. Olympus FV10 ASW 1.7 software was used for acquisition of the images.

4.8. Statistical Analysis

Statistical analysis of cytotoxicity and spectral data was performed using the Student's t-test Origin 2022 software (OriginLab Corporation). Values are given as the mean ± SD of three or five experiments.

Supplementary Materials: The following supporting information can be downloaded at the website of this paper posted on Preprints.org, Figure S1. FTIR spectra of Chit5, LA, its conjugate Chit5-LA. PBS (0.01 M, pH 7.4). T = 22 °C. Figure S2. Zoomed FTIR spectra of Chit5-LA and DoxMC2 (Dox-SS-LA-Chit5) in the wavenumber region 2650-2450 cm^{-1}. PBS (0.01 M, pH 7.4). T = 22 °C. Figure S3. FTIR spectra of normal HEK293T cells during incubation for 30 min with free Dox (0.1 mg/mL) and micellar Dox formulation (DoxM1). PBS (0.01 M, pH = 7.4). T = 22 or 37 °C. Figure S4. ^1H NMR of Chit5 grafted with (a) lipoic acid and (b) oleic acid. PBS (0.01M, pH = 7.4). T = 22 °C.

Author Contributions: Conceptualization, E.V.K., I.D.Z; methodology, I.D.Z., E.V.K., A.A.E., N.V.D.; formal analysis, I.D.Z.; investigation, I.D.Z, A.A.E., N.V.D.; data curation, I.D.Z.; writing—original draft preparation, I.D.Z.; writing—review and editing, E.V.K; project supervision, E.V.K.; funding acquisition, E.V.K. All authors have read and agreed to the published version of the manuscript.

Funding: This research was funded by the Russian Science Foundation, grant number 24-25-00104.

Institutional Review Board Statement: Cell lines were obtained from Lomonosov Moscow State University Depository of Live Systems Collection (Moscow, Russia): Raji, K562, A875 cells.

Informed Consent Statement: Not applicable.

Data Availability Statement: The data presented in this study are available in the main text and Supplementary Materials.

Acknowledgments: The work was performed using the equipment (FTIR microscope MICRAN-3, FTIR spectrometer Bruker Tensor 27, Jasco J-815 CD Spectrometer, AFM microscope NTEGRA II – of the program for the development of Moscow State University.

Conflicts of Interest: The authors declare no conflict of interest.

Abbreviations

Chit – chitosan; CLSM – confocal laser scanning microscopy; Dox – doxorubicin; EDC – 1-Ethyl-3-(3-dimethylaminopropyl) carbodiimide; FTIR – Fourier transformed infrared; GSH –reduced glutathione; GSSG – oxidized glutathione; Hep – heparin; LA – lipoic acid; NHS – N-hydroxysuccinimide; OA – oleic acid.

References

1. Mavromoustakos, T.; Tzakos, A.G. *Supramolecules in Drug Discovery and Drug Delivery*; ISBN 9781071609194.
2. Buranachai, T.; Praphairaksit, N.; Muangsin, N. Chitosan/polyethylene glycol beads crosslinked with tripolyphosphate and glutaraldehyde for gastrointestinal drug delivery. *AAPS PharmSciTech* **2010**, *11*, 1128–1137. https://doi.org/10.1208/s12249-010-9483-z.
3. Liu, Z.; Jiao, Y.; Wang, Y.; Zhou, C.; Zhang, Z. Polysaccharides-based nanoparticles as drug delivery systems. *Adv. Drug Deliv. Rev.* **2008**, *60*, 1650–1662. https://doi.org/10.1016/j.addr.2008.09.001.
4. Haimhoffer, Á.; Rusznyák, Á.; Réti-Nagy, K.; Vasvári, G.; Váradi, J.; Vecsernyés, M.; Bácskay, I.; Fehér, P.; Ujhelyi, Z.; Fenyvesi, F. Cyclodextrins in drug delivery systems and their effects on biological barriers. *Sci. Pharm.* **2019**, *87*. https://doi.org/10.3390/scipharm87040033.
5. Stebbins, N.D.; Ouimet, M.A.; Uhrich, K.E. Antibiotic-containing polymers for localized, sustained drug delivery. *Adv. Drug Deliv. Rev.* **2014**, *78*, 77–87. https://doi.org/10.1016/j.addr.2014.04.006.
6. Cho, K.; Wang, X.; Nie, S.; Chen, Z.; Shin, D.M. Therapeutic nanoparticles for drug delivery in cancer. *Clin. Cancer Res.* **2008**, *14*, 1310–1316. https://doi.org/10.1158/1078-0432.CCR-07-1441.
7. Loftsson, T.; Jarho, P.; Másson, M.; Järvinen, T. Cyclodextrins in drug delivery system. *Expert Opin. Drug Deliv.* **2005**, *2*, 335–346. https://doi.org/10.1016/S0169-409X(98)00051-9.
8. Zlotnikov, I.D.; Kudryashova, E. V. Computer simulation of the Receptor–Ligand Interactions of Mannose Receptor CD206 in Comparison with the Lectin Concanavalin A Model. *Biochem.* **2022**, *87*, 54–69. https://doi.org/10.1134/S0006297922010059.
9. Cavalcante, C.H.; Fernandes, R.S.; de Oliveira Silva, J.; Ramos Oda, C.M.; Leite, E.A.; Cassali, G.D.; Charlie-Silva, I.; Ventura Fernandes, B.H.; Miranda Ferreira, L.A.; de Barros, A.L.B. Doxorubicin-loaded pH-sensitive micelles: A promising alternative to enhance antitumor activity and reduce toxicity. *Biomed. Pharmacother.* **2021**, *134*. https://doi.org/10.1016/j.biopha.2020.111076.
10. Gonzalez-Fajardo, L.; Mahajan, L.H.; Ndaya, D.; Hargrove, D.; Manautou, J.E.; Liang, B.T.; Chen, M.H.; Kasi, R.M.; Lu, X. Reduced in vivo toxicity of doxorubicin by encapsulation in cholesterol-containing self-assembled nanoparticles. *Pharmacol. Res.* **2016**, *107*, 93–101. https://doi.org/10.1016/j.phrs.2016.03.006.
11. Tammam, S.N.; Azzazy, H.M.E.; Breitinger, H.G.; Lamprecht, A. Chitosan Nanoparticles for Nuclear Targeting: The Effect of Nanoparticle Size and Nuclear Localization Sequence Density. *Mol. Pharm.* **2015**, *12*, 4277–4289. https://doi.org/10.1021/acs.molpharmaceut.5b00478.
12. Zhong, P.; Zhang, J.; Deng, C.; Cheng, R.; Meng, F.; Zhong, Z. Glutathione-Sensitive Hyaluronic Acid-SS-Mertansine Prodrug with a High Drug Content: Facile Synthesis and Targeted Breast Tumor Therapy. *Biomacromolecules* **2016**, *17*, 3602–3608. https://doi.org/10.1021/acs.biomac.6b01094.
13. Bagheri, M.; Validi, M.; Gholipour, A.; Makvandi, P.; Sharifi, E. Chitosan nanofiber biocomposites for potential wound healing applications: Antioxidant activity with synergic antibacterial effect. *Bioeng. Transl. Med.* **2022**, *7*, 1–15. https://doi.org/10.1002/btm2.10254.
14. Serra, P.; Santamaria, P. Nanoparticle-based autoimmune disease therapy. *Clin. Immunol.* **2015**, *160*, 3–13. https://doi.org/10.1016/j.clim.2015.02.003.
15. Yang, C.; Gao, S.; Dagnæs-Hansen, F.; Jakobsen, M.; Kjems, J. Impact of PEG Chain Length on the Physical Properties and Bioactivity of PEGylated Chitosan/siRNA Nanoparticles in Vitro and in Vivo. *ACS Appl. Mater. Interfaces* **2017**, *9*, 12203–12216. https://doi.org/10.1021/acsami.6b16556.
16. Mahor, S.; Dash, B.C.; O'Connor, S.; Pandit, A. Mannosylated polyethyleneimine-hyaluronan nanohybrids for targeted gene delivery to macrophage-like cell lines. *Bioconjug. Chem.* **2012**, *23*, 1138–1148. https://doi.org/10.1021/bc200599k.
17. Huang, H.J.; Tsai, Y.L.; Lin, S.H.; Hsu, S.H. Smart polymers for cell therapy and precision medicine. *J. Biomed. Sci.* **2019**, *26*, 1–11. https://doi.org/10.1186/s12929-019-0571-4.
18. Psimadas, D.; Georgoulias, P.; Valotassiou, V.; Loudos, G. Molecular Nanomedicine Towards Cancer : *J. Pharm. Sci.* **2012**, *101*, 2271–2280. https://doi.org/10.1002/jps.
19. Negut, I.; Bita, B. Polymeric Micellar Systems—A Special Emphasis on "Smart" Drug Delivery. *Pharmaceutics* **2023**, *15*. https://doi.org/10.3390/pharmaceutics15030976.
20. Raval, N.; Maheshwari, R.; Shukla, H.; Kalia, K.; Torchilin, V.P.; Tekade, R.K. Multifunctional polymeric micellar nanomedicine in the diagnosis and treatment of cancer. *Mater. Sci. Eng. C* **2021**, *126*, 112186. https://doi.org/10.1016/j.msec.2021.112186.

21. Vaupel, P.; Kallinowski, F.; Okunieff, P. Blood Flow, Oxygen and Nutrient Supply, and Metabolic Microenvironment of Human Tumors: A Review. *Cancer Res.* **1989**, *49*, 6449–6465.
22. Ray, P.; Confeld, M.; Borowicz, P.; Wang, T.; Mallik, S.; Quadir, M. *PEG-b-poly (carbonate)-derived nanocarrier platform with pH-responsive properties for pancreatic cancer combination therapy*; Elsevier B.V., 2019; T. 174; ISBN 7012318333.
23. Ngan, V.T.T.; Chiou, P.Y.; Ilhami, F.B.; Bayle, E.A.; Shieh, Y.T.; Chuang, W.T.; Chen, J.K.; Lai, J.Y.; Cheng, C.C. A CO2-Responsive Imidazole-Functionalized Fluorescent Material Mediates Cancer Chemotherapy. *Pharmaceutics* **2023**, *15*. https://doi.org/10.3390/pharmaceutics15020354.
24. Wang, Z.; Deng, X.; Ding, J.; Zhou, W.; Zheng, X.; Tang, G. Mechanisms of drug release in pH-sensitive micelles for tumour targeted drug delivery system: A review. *Int. J. Pharm.* **2018**, *535*, 253–260. https://doi.org/10.1016/j.ijpharm.2017.11.003.
25. Junnuthula, V.; Kolimi, P.; Nyavanandi, D.; Sampathi, S.; Vora, L.K.; Dyawanapelly, S. Polymeric Micelles for Breast Cancer Therapy: Recent Updates, Clinical Translation and Regulatory Considerations. *Pharmaceutics* **2022**, *14*. https://doi.org/10.3390/pharmaceutics14091860.
26. He, L.; Qin, X.; Fan, D.; Feng, C.; Wang, Q.; Fang, J. Dual-Stimuli Responsive Polymeric Micelles for the Effective Treatment of Rheumatoid Arthritis. *ACS Appl. Mater. Interfaces* **2021**, *13*, 21076–21086. https://doi.org/10.1021/acsami.1c04953.
27. Mutlu-Agardan, N.B.; Sarisozen, C.; Torchilin, V.P. Cytotoxicity of Novel Redox Sensitive PEG2000-S-S-PTX Micelles against Drug-Resistant Ovarian and Breast Cancer Cells. *Pharm. Res.* **2020**, *37*. https://doi.org/10.1007/s11095-020-2759-4.
28. Wang, L.; Li, C. PH responsive fluorescence nanoprobe imaging of tumors by sensing the acidic microenvironment. *J. Mater. Chem.* **2011**, *21*, 15862–15871. https://doi.org/10.1039/c1jm12072g.
29. Ribeiro, I.S.; Leornado, A.L.S.; Carneiro, M.J.M.; Filho, R.N.C.; Freire, R.S. pH-responsive prodrug nanoparticles based cashew gum as a doxorubicin delivery sys- tem. **2022**, 1–18.
30. Zlotnikov, I.D.; Dobryakova, N. V.; Ezhov, A.A.; Kudryashova, E. V. Achievement of the Selectivity of Cytotoxic Agents against Cancer Cells by Creation of Combined Formulation with Terpenoid Adjuvants as Prospects to Overcome Multidrug Resistance. *Int. J. Mol. Sci.* **2023**, *24*, 1–34. https://doi.org/10.3390/ijms24098023.
31. Zlotnikov, I.D.; Streltsov, D.A.; Ezhov, A.A.; Kudryashova, E. V. Smart pH- and Temperature-Sensitive Micelles Based on Chitosan Grafted with Fatty Acids to Increase the Efficiency and Selectivity of Doxorubicin and Its Adjuvant Regarding the Tumor Cells. *Pharmaceutics* **2023**, *15*. https://doi.org/10.3390/pharmaceutics15041135.
32. Li, C.; Xia, J.; Wei, X.; Yan, H.; Si, Z.; Ju, S. PH-Activated near-infrared fluorescence nanoprobe imaging tumors by sensing the acidic microenvironment. *Adv. Funct. Mater.* **2010**, *20*, 2222–2230. https://doi.org/10.1002/adfm.201000038.
33. Huo, M.; Liu, Y.; Wang, L.; Yin, T.; Qin, C.; Xiao, Y.; Yin, L.; Liu, J.; Zhou, J. *Redox-Sensitive Micelles Based on O,N-Hydroxyethyl Chitosan-Octylamine Conjugates for Triggered Intracellular Delivery of Paclitaxel*; 2016; T. 13; ISBN 8621311623.
34. Luo, T.; Han, J.; Zhao, F.; Pan, X.; Tian, B.; Ding, X.; Zhang, J. Redox-sensitive micelles based on retinoic acid modified chitosan conjugate for intracellular drug delivery and smart drug release in cancer therapy. *Carbohydr. Polym.* **2019**, *215*, 8–19. https://doi.org/10.1016/j.carbpol.2019.03.064.
35. Shim, W.S.; Kim, J.H.; Kim, K.; Kim, Y.S.; Park, R.W.; Kim, I.S.; Kwon, I.C.; Lee, D.S. pH- and temperature-sensitive, injectable, biodegradable block copolymer hydrogels as carriers for paclitaxel. *Int. J. Pharm.* **2007**, *331*, 11–18. https://doi.org/10.1016/j.ijpharm.2006.09.027.
36. Wu, J.; Su, Z.; Ma, G. A thermo- and pH-sensitive hydrogel composed of quaternized chitosan / glycerophosphate. **2006**, *315*, 1–11. https://doi.org/10.1016/j.ijpharm.2006.01.045.
37. Liow, S.S.; Dou, Q.; Kai, D.; Karim, A.A.; Zhang, K.; Xu, F.; Loh, X.J. Thermogels: In Situ Gelling Biomaterial. *ACS Biomater. Sci. Eng.* **2016**, *2*, 295–316. https://doi.org/10.1021/acsbiomaterials.5b00515.
38. Takei, T.; Nakahara, H.; Ijima, H.; Kawakami, K. Synthesis of a chitosan derivative soluble at neutral pH and gellable by freeze-thawing, and its application in wound care. *Acta Biomater.* **2012**, *8*, 686–693. https://doi.org/10.1016/j.actbio.2011.10.005.
39. Falanga, A.; Russo, L.; Verzeroli, C. Mechanisms of thrombosis in cancer. *Thromb. Res.* **2013**, *131*, S59–S62. https://doi.org/10.1016/S0049-3848(13)70024-0.
40. Falanga, A.; Russo, L.; Milesi, V.; Vignoli, A. Mechanisms and risk factors of thrombosis in cancer. *Crit. Rev. Oncol. Hematol.* **2017**, *118*, 79–83. https://doi.org/10.1016/j.critrevonc.2017.08.003.
41. Young, A.; Chapman, O.; Connor, C.; Poole, C.; Rose, P.; Kakkar, A.K. Thrombosis and cancer. *Nat. Rev. Clin. Oncol.* **2012**, *9*, 437–449. https://doi.org/10.1038/nrclinonc.2012.106.
42. Cunningham, R.S. The Role of Low-Molecular-Weight Heparins as Supportive Care Therapy in Cancer-Associated Thrombosis. *Semin. Oncol.* **2006**, *33*, 17–25. https://doi.org/10.1053/j.seminoncol.2006.01.022.
43. Devlin, A.; Mauri, L.; Guerrini, M.; Yates, E.A.; Skidmore, M.A. The use of ATR-FTIR spectroscopy to characterise crude heparin samples by composition and structural features. *bioRxiv* **2019**, 744532.

44. Martins, A.F.; Piai, J.F.; Schuquel, I.T.A.; Rubira, A.F.; Muniz, E.C. Polyelectrolyte complexes of chitosan/heparin and N,N,N-trimethyl chitosan/heparin obtained at different pH: I. Preparation, characterization, and controlled release of heparin. *Colloid Polym. Sci.* **2011**, *289*, 1133–1144. https://doi.org/10.1007/s00396-011-2437-5.
45. Lundin, M.; Blomberg, E.; Tilton, R.D. Polymer dynamics in layer-by-layer assemblies of chitosan and heparin. *Langmuir* **2010**, *26*, 3242–3251. https://doi.org/10.1021/la902968h.
46. Harada, N.S.; Oyama, H.T.; Bártoli, J.R.; Gouvêa, D.; Cestari, I.A.; Wang, S.H. Quantifying adsorption of heparin on a PVC substrate using ATR-FTIR. *Polym. Int.* **2005**, *54*, 209–214. https://doi.org/10.1002/pi.1685.
47. Fischer, E.G. Nuclear Morphology and the Biology of Cancer Cells. *Acta Cytol.* **2020**, *64*, 511–519. https://doi.org/10.1159/000508780.
48. Balendiran, G.K.; Dabur, R.; Fraser, D. The role of glutathione in cancer. *Cell Biochem. Funct.* **2004**, *22*, 343–352. https://doi.org/10.1002/cbf.1149.
49. Kennedy, L.; Sandhu, J.K.; Harper, M.E.; Cuperlovic-culf, M. Role of glutathione in cancer: From mechanisms to therapies. *Biomolecules* **2020**, *10*, 1–27. https://doi.org/10.3390/biom10101429.
50. Valtis, Y.K.; Flamand, Y.; Shimony, S.; Place, A.E.; Silverman, L.B.; Vrooman, L.M.; Brunner, A.M.; Sallan, S.E.; Wadleigh, M.; Stone, R.M.; *и др.* Treatment completion, asparaginase completion, and oncologic outcomes among children, adolescents and young adults with acute lymphoblastic leukemia treated with DFCI Consortium Protocols. *Leukemia* **2024**. https://doi.org/10.1038/s41375-023-02115-4.
51. Yao, H.; Zhang, C.; Tan, X.; Li, J.; Yin, X.; Deng, X.; Chen, T.; Rao, J.; Gao, L.; Kong, P.; *и др.* Efficacy and toxicity of CLAG combined with pegylated liposomal doxorubicin in the treatment of refractory or relapsed acute myeloid leukemia. *Cancer Med.* **2023**, *12*, 12377–12387. https://doi.org/10.1002/cam4.5938.
52. Vrooman, L.M.; Blonquist, T.M.; Harris, M.H.; Stevenson, K.E.; Place, A.E.; Hunt, S.K.; O'Brien, J.E.; Asselin, B.L.; Athale, U.H.; Clavell, L.A.; *и др.* Refining risk classification in childhood b acute lymphoblastic leukemia: Results of DFCI ALL consortium protocol 05-001. *Blood Adv.* **2018**, *2*, 1449–1458. https://doi.org/10.1182/bloodadvances.2018016584.
53. Egler, R.A.; Ahuja, S.P.; Matloub, Y. L-asparaginase in the treatment of patients with acute lymphoblastic leukemia. *J. Pharmacol. Pharmacother.* **2016**, *7*, 62–71. https://doi.org/10.4103/0976-500X.184769.
54. Shadman, M. Diagnosis and Treatment of Chronic Lymphocytic Leukemia: A Review. *Jama* **2023**, *329*, 918–932. https://doi.org/10.1001/jama.2023.1946.
55. Wu, X.; Chen, S.; Huang, K.; Lin, G. Triptolide promotes ferroptosis by suppressing Nrf2 to overcome leukemia cell resistance to doxorubicin. *Mol. Med. Rep.* **2023**, *27*, 1–8. https://doi.org/10.3892/mmr.2022.12904.
56. Zlotnikov, I.D.; Ezhov, A.A.; Vigovskiy, M.A.; Grigorieva, O.A.; Dyachkova, U.D.; Belogurova, N.G.; Kudryashova, E. V. Application Prospects of FTIR Spectroscopy and CLSM to Monitor the Drugs Interaction with Bacteria Cells Localized in Macrophages for Diagnosis and Treatment Control of Respiratory Diseases. *Diagnostics* **2023**, *13*, 1–23. https://doi.org/10.3390/diagnostics13040698.
57. Zlotnikov, I.D.; Vigovskiy, M.A.; Davydova, M.P.; Danilov, M.R.; Dyachkova, U.D.; Grigorieva, O.A.; Kudryashova, E. V. Mannosylated Systems for Targeted Delivery of Antibacterial Drugs to Activated Macrophages. *Int. J. Mol. Sci.* **2022**, *23*, 1–29. https://doi.org/10.3390/ijms232416144.